

TECHNICAL RESEARCH REPORT

Discrete-Time Integral Control of PWM DC-DC Converters

by C.-C. Fang, E.H. Abed

T.R. 98-52



ISR develops, applies and teaches advanced methodologies of design and analysis to solve complex, hierarchical, heterogeneous and dynamic problems of engineering technology and systems for industry and government.

ISR is a permanent institute of the University of Maryland, within the Glenn L. Martin Institute of Technology/A. James Clark School of Engineering. It is a National Science Foundation Engineering Research Center.

Web site <http://www.isr.umd.edu>

Discrete-Time Integral Control of PWM DC-DC Converters

Chung-Chieh Fang and Eyad H. Abed*
Department of Electrical Engineering
and the Institute for Systems Research
University of Maryland
College Park, MD 20742 USA
ccfang@isr.umd.edu, abed@isr.umd.edu

Manuscript:

Abstract

Discrete-time integral control of the PWM DC-DC converters is considered using recently developed general sampled-data power stage models. Either the voltage or current of the power stage can be controlled. Both state feedback and output feedback are addressed. Line and load regulation are achieved through a discrete-time integrator. By adding an analog filter, the average value of output can be regulated. For converters belonging to a certain class, state observers are constructed.

1 Introduction

A DC-DC converter consists of a power stage and a controller, as shown in Fig. 1. The main objectives of the controller design are *(i)* stability, *(ii)* fast transient dynamics, *(iii)* satisfactory line regulation, and *(iv)* satisfactory load regulation.

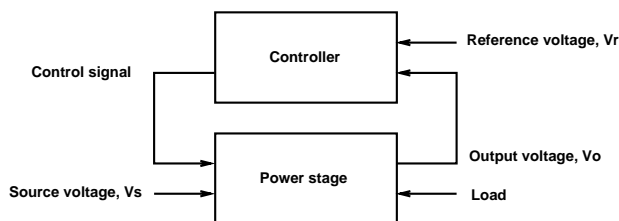


Figure 1: System diagram of a DC-DC converter

In this paper, discrete-time integral control of PWM DC-DC converters is studied. Controllers are designed using the sampled-data power stage model recently developed by the authors [1, 5].

*Corresponding author

This model has been shown to be more accurate than the traditional averaged models. In the sampled-data model, capacitor voltages and inductor currents are considered as state variables and either of them can be controlled by the proposed controller design. Also, the sampled-data model is sufficiently general that either peak or averaged state values can be controlled. Both state feedback and output feedback are addressed. For a special class of converters, state observers are constructed.

The proposed controller design method differs from the traditional approach. In the traditional design approach, the power stage is modeled and analyzed by averaging methods [2, 3, 4]. Based on the averaged model, a controller is designed. Then simulation programs are used to test the closed-loop performance. For a review of different controller designs based on averaged models, see [5].

The remainder of the paper is organized as follows. In Section 2, a general power stage model for PWM DC-DC converters developed by the authors in [1, 5] is reviewed. In Section 3, closed-loop structure of discrete-time control is addressed. In Section 4, a scheme to control average output by adding an analog filter is proposed. In Section 5 and Section 7, state feedback and output feedback are addressed respectively. In Section 6, discrete-time state observers for some special converters are proposed. In Section 8, four illustrative examples are given. Conclusions are collected in Section 9.

2 General Sampled-Data Model for PWM Converter Power Stage

In this section, a summary of the sampled-data modeling of a PWM converter power stage in [1, 5] is given. Here and throughout the paper, the converter is assumed to be operating in continuous conduction mode. The results readily extend to discontinuous conduction mode. The summary below includes a general block diagram model as well as associated nonlinear and linearized sampled-data models.

Let the switching instant be the control variable. Equivalently, the duty cycle can be considered the control variable. A block diagram model for a PWM converter power stage in continuous conduction mode is shown in Fig. 2, where $d_n \in \mathbf{R}$ is the switching instant within the cycle,

$A_1, A_2 \in \mathbf{R}^{N \times N}$, $B_1, B_2 \in \mathbf{R}^{N \times 1}$, $F_1, F_2 \in \mathbf{R}^{1 \times N}$, are constant matrices, T is the constant switching period (inverse of switching frequency f_s), $v_s \in \mathbf{R}$ is the source voltage, and $w \in \mathbf{R}$ is the output. A typical output can be output voltage, output current, or inductor current.

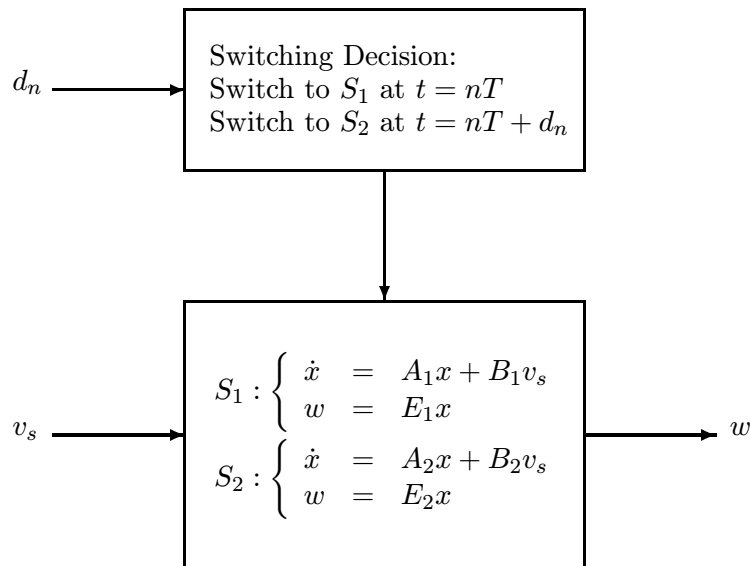


Figure 2: Power stage of PWM converter in continuous conduction mode

The two matrices E_1 and E_2 need not be the same. When they differ, the output signal is discontinuous. In the following, E is used to denote either E_1 , E_2 , or $(E_1 + E_2)/2$ depending on which output value is of interest.

Take v_s to be constant within the cycle and denote it as v_{sn} . Let $x_n = x(nT)$ and $w_n = z(nT)$. From the operation in Fig. 2, the sampled-data dynamics of the power stage is

$$\begin{aligned}
 x_{n+1} &= f(x_n, v_{sn}, d_n) \\
 &= e^{A_2(T-d_n)}(e^{A_1d_n}x_n + \int_0^{d_n} e^{A_1\sigma}d\sigma B_1v_{sn}) + \int_0^{T-d_n} e^{A_2\sigma}d\sigma B_2v_{sn} \\
 w_n &= Ex_n
 \end{aligned} \tag{1}$$

Let the nominal (set-point) controlled output be W_{SET} and steady-state state orbit be $x^0(t)$. Let the fixed point of the system (1) be $(x^0(0), V_s, d)$. Then the system (1) has the linearized dynamics

$$\begin{aligned}
 \hat{x}_{n+1} &\approx \Phi_o \hat{x}_n + \Gamma_v \hat{v}_{sn} + \Gamma_d \hat{d}_n \\
 \hat{w}_n &= E \hat{x}_n
 \end{aligned} \tag{2}$$

where

$$\Phi_o = e^{A_2(T-d)} e^{A_1 d} \quad (3)$$

$$\Gamma_v = e^{A_2(T-d)} \int_0^d e^{A_1 \sigma} d\sigma B_1 + \int_0^{T-d} e^{A_2 \sigma} d\sigma B_2 \quad (4)$$

$$\begin{aligned} \Gamma_d &= e^{A_2(T-d)} ((A_1 - A_2)x^0(d) + (B_1 - B_2)V_s) \\ &= e^{A_2(T-d)} (\dot{x}^0(d^-) - \dot{x}^0(d^+)) \end{aligned} \quad (5)$$

The eigenvalues of matrix Φ_o determines the open-loop stability. Under the assumption that A_1 and A_2 have no eigenvalues with positive real part, and that at least one of these matrices has all eigenvalues with negative real part, it can be proved that all of the eigenvalues of matrix Φ_o are inside the unit circle and thus the power stage is open-loop stable.

The open-loop audio-susceptibility and output impedance in the z -domain can be derived from Eq. (1). The results can be found in [1]. The corresponding effective frequency responses [6, p. 93], valid in the frequency range $|\omega| < \frac{\pi}{T}$, can be derived by replacing z by $e^{j\omega T}$ in the results [1].

The effect of a line disturbance on the output can be seen from Eq. (2). To study the effect of a load disturbance, add a fictitious current source, i_o (as perturbation), in parallel with the load. Let

$$\begin{aligned} S_1 : \dot{x} &= A_1 x + B_1 v_s + B_{i1} i_o \\ S_2 : \dot{x} &= A_1 x + B_2 v_s + B_{i2} i_o \end{aligned} \quad (6)$$

where $B_{i1}, B_{i2} \in \mathbf{R}^{N \times 1}$ are constant matrices. From Eq. (6), line and load disturbances affect the dynamics through matrices B_1, B_2 and B_{i1}, B_{i2} respectively. Similar to Γ_v in Eq. (4), a term related to output impedance can be defined:

$$\Gamma_i = e^{A_2(T-d)} \int_0^d e^{A_1 \sigma} d\sigma B_{i1} + \int_0^{T-d} e^{A_2 \sigma} d\sigma B_{i2} \quad (7)$$

3 Closed-Loop Structure of Discrete-Time Control

Given the power stage in Section 2, the implementation of discrete-time control is done by adding feedback and feedforward paths. In state feedback, the state x is used; in output feedback, measured

state variables $y \in \mathbf{R}^M$ ($M \leq N$) are used. The feedforward path does not affect closed-loop stability and is optional in some cases. When it is used, the transient response is improved. The resulting system diagram is shown in Fig. 3, where $C \in \mathbf{R}^{M \times N}$ is a constant matrix.

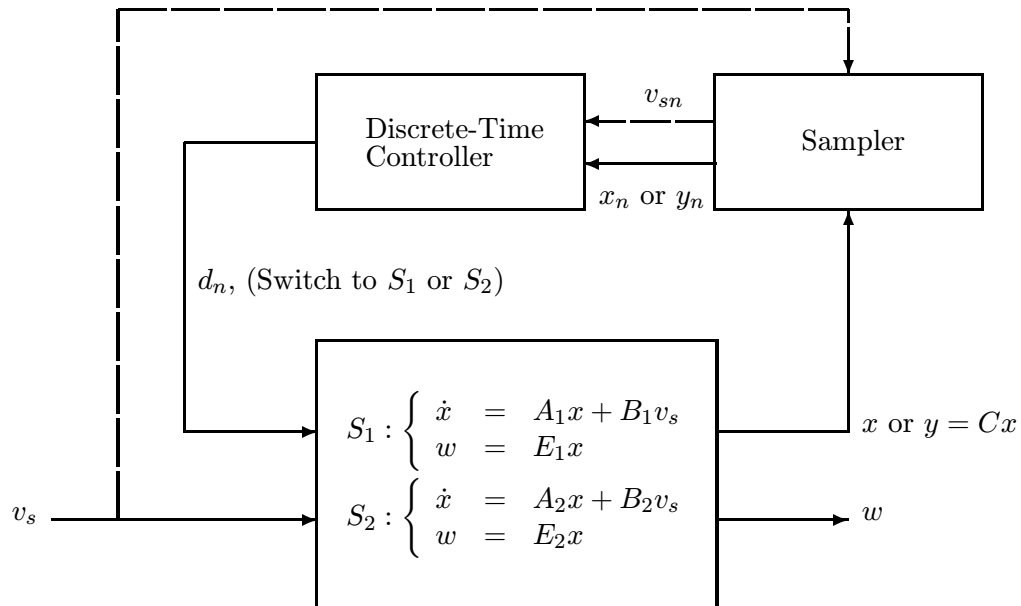


Figure 3: Power stage of PWM converter and discrete-time controller

There is a natural constraint that applies when using d_n as the control variable, because d_n must be between 0 and T . To implement the controller, we need to add a limiter ℓ on d_n , where

$$\ell(t) = \begin{cases} 0 & \text{for } t < 0 \\ t & \text{for } t \in [0, T] \\ T & \text{for } t > T \end{cases} \quad (8)$$

Since here the local dynamics is emphasized, the limiter is not shown explicitly.

4 Control of Average Output

In discrete-time control, the controlled output is sampled at $t = nT$. So only the sampled value of the output is controlled. The value could be the maximum, minimum or in-between in a cycle. Sometimes it is desired that the *average* output is controlled, but the sampled output (at $t = nT$) is the *maximum* value (for example, the signal on the left hand side of Fig. 4). In this case, a

1-dimensional *analog* low-pass filter can be applied to that state. Since the filter is analog, it can be considered to be part of the power stage and augments the dimension of power stage from N to $N + 1$ without extra modeling effort. This also shows the usefulness of modeling of the power stage in a general way as in Section 2. The effect of a low-pass filter is shown in Fig. 4. The filter reduces the ripple, filters out the average value, and shifts the phase. Since the filtered signal is sampled and fed back, the average output can be controlled. This is at the expense of requiring an additional measurement. An example of average current control will be given in Section 8.

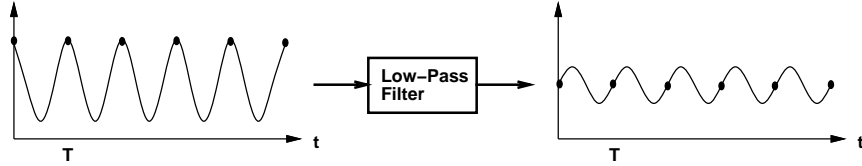


Figure 4: Adding a low-pass filter to reduce the ripple, filter out the average value and shift the phase

5 State Feedback Integral Control (SFIC)

Integral control is commonly used to reduce steady-state errors. In DC-DC conversion, one of the main objectives is to regulate the output voltage or current. This motivates the use of integral control in this paper.

The state feedback integral controller (SFIC) proposed for the PWM converter is a dynamic controller with input x_n and output d_n :

$$v_{n+1} = v_n + W_{\text{SET}} - Ex_n \quad (9)$$

$$d_n = -K_1x_n - K_2v_n \quad (10)$$

Here, $v_n \in \mathbf{R}$ is the integrator state, and $K_1 \in \mathbf{R}^{1 \times n}$, $K_2 \in \mathbf{R}$ are the feedback gains.

Let the fixed point be $(x_n, v_{sn}, d_n, v_n) = (x^0(0), V_s, d, v)$. From Eq. (9), $Ex^0(0) = W_{\text{SET}}$ in steady state. So the controller automatically drives the output Ex to W_{SET} if the feedback gains are chosen to ensure stability.

From Eqs. (2) and (9), the linearized dynamics of the closed-loop system is

$$\begin{aligned} \begin{bmatrix} \hat{x}_{n+1} \\ \hat{v}_{n+1} \end{bmatrix} &\approx \begin{bmatrix} \Phi_o & 0 \\ -E & 1 \end{bmatrix} \begin{bmatrix} \hat{x}_n \\ \hat{v}_n \end{bmatrix} + \begin{bmatrix} \Gamma_d \\ 0 \end{bmatrix} \hat{d}_n + \begin{bmatrix} \Gamma_v \\ 0 \end{bmatrix} \hat{v}_{sn} \\ \hat{w}_n &= E\hat{x}_n \end{aligned} \quad (11)$$

Next, a sufficient condition is given for the stability of the closed-loop system.

Theorem 1 *Assume that A_1 and A_2 have no eigenvalues with positive real part, and that at least one of these matrices has all eigenvalues with negative real part. If the matrix $\begin{bmatrix} \Phi_o - I & \Gamma_d \\ E & 0 \end{bmatrix}$ is of full rank, then the power stage model (1) is asymptotically stabilizable by using state feedback integral control.*

Proof:

All the eigenvalues of Φ are inside the unit circle. So one just needs to prove that the eigenvalue at 1, which is introduced by the integral control, is controllable. By the PBH rank test [7], this is true if the matrix $\begin{bmatrix} \Phi_o - I & \Gamma_d \\ E & 0 \end{bmatrix}$ is of full rank. \square

The degree of line and load regulation achieved with control can be discerned from the closed-loop audio-susceptibility and output impedance, which are derived next. From Eq. (11), the audio-susceptibility of the closed-loop system is

$$T_{os}(z) = \frac{\hat{w}(z)}{\hat{v}_s(z)} = \begin{bmatrix} E & 0 \end{bmatrix} (zI - \begin{bmatrix} \Phi_o & 0 \\ -E & 1 \end{bmatrix} + \begin{bmatrix} \Gamma_d \\ 0 \end{bmatrix} \begin{bmatrix} K_1 & K_2 \end{bmatrix})^{-1} \begin{bmatrix} \Gamma_v \\ 0 \end{bmatrix} \quad (12)$$

Similarly, the output impedance of the closed-loop system is

$$T_{oo}(z) = \frac{\hat{w}(z)}{\hat{i}_o(z)} = \begin{bmatrix} E & 0 \end{bmatrix} (zI - \begin{bmatrix} \Phi_o & 0 \\ -E & 1 \end{bmatrix} + \begin{bmatrix} \Gamma_d \\ 0 \end{bmatrix} \begin{bmatrix} K_1 & K_2 \end{bmatrix})^{-1} \begin{bmatrix} \Gamma_i \\ 0 \end{bmatrix} \quad (13)$$

6 Discrete-Time State Observer Design in the Case $A_1 = A_2$

In state feedback controller designs, all of the states are assumed to be measurable. The states are either voltages or currents. Generally current measurement is noisier than voltage measurement

[8, page 3.153]. It is desired that only voltage is measured and fed back for compensation while maintaining the performance level achievable with full state feedback. In this section, a state observer for the case $A_1 = A_2$ will be derived.

In [9], the authors designed a state observer from an averaged model, which is an approximate model. Here, however, a state observer is designed for the sampled-data model, which is a highly accurate model. In [10], an extra measurement of the inductor voltage is used to get the inductor current.

Some converters, like buck converters [5], satisfy $A_1 = A_2 =: A$. Then the sampled-data dynamics of the power stage is

$$\begin{aligned} x_{n+1} &= e^{AT} x_n + e^{A(T-d_n)} \int_0^{d_n} e^{A\sigma} d\sigma B_1 v_{sn} + \int_0^{T-d_n} e^{A\sigma} d\sigma B_2 v_{sn} \\ &=: \Theta x_n + \Lambda(d_n, v_{sn}) \end{aligned} \quad (14)$$

where $\Theta = e^{AT}$.

A full-order observer and a reduced-order observer are given next.

6.1 Full-Order State Observer

The proposed full-order observer is

$$z_{n+1} = \Theta z_n + \Lambda(d_n, v_{sn}) + G(y_n - C z_n) \quad (15)$$

where $z \in \mathbf{R}^N$ is the state of the observer and $G \in \mathbf{R}^{N \times M}$ is a feedback gain matrix.

Letting $e_n = x_n - z_n$ be the error between the real state and the observer state, and subtracting Eq. (15) from Eq. (14) gives

$$e_{n+1} = (\Theta - GC)e_n \quad (16)$$

Thus the error dynamics is linear.

Generally all of the eigenvalues of A have negative real part under the assumptions stated in Section 2, so all of the eigenvalues of $\Theta = e^{AT}$ lie within the unit circle. Thus, the pair (Θ', C') is stabilizable, and there exists an observer which asymptotically tracks the state of system (14).

6.2 Reduced-Order State Observer

In Section 6.1, both the unmeasured and measured states are estimated, while in fact the measured states are already available. To estimate just the unmeasured states, a reduced-order state observer can be designed. Without loss of generality, the first M states of the output are assumed to be measurable, so $C = [I, 0]$, where I is an $M \times M$ identity matrix. Then Eq. (14) can be decomposed into

$$\begin{bmatrix} y_{n+1} \\ u_{n+1} \end{bmatrix} = \begin{bmatrix} \Theta_{11} & \Theta_{12} \\ \Theta_{21} & \Theta_{22} \end{bmatrix} \begin{bmatrix} y_n \\ u_n \end{bmatrix} + \begin{bmatrix} \Lambda_1(d_n, v_{sn}) \\ \Lambda_2(d_n, v_{sn}) \end{bmatrix} \quad (17)$$

where $y_n \in \mathbf{R}^M$ is the measured state and $u_n \in \mathbf{R}^{N-M}$ is the unmeasured state.

The proposed reduced-order observer has the following structure:

$$z_{n+1} = (\Theta_{22} - G\Theta_{12})z_n + \Theta_{21}y_n + \Lambda_2(d_n, v_{sn}) + G(y_{n+1} - \Theta_{11}y_n - \Lambda_1(d_n, v_{sn}))$$

Here $z \in \mathbf{R}^{N-M}$ is the state of the reduced-order observer and $G \in \mathbf{R}^{(N-M) \times M}$ is a feedback gain matrix. Letting $e_n =: u_n - z_n$, one has

$$e_{n+1} = (\Theta_{22} - G\Theta_{12})e_n \quad (18)$$

Thus, if the pair $(\Theta'_{22}, \Theta'_{12})$ is stabilizable, then there exists a reduced-order observer which asymptotically tracks the unmeasured state in the system (14).

7 Output Feedback Integral Control

For other converters with $A_1 \neq A_2$, it can be demonstrated that given partial measured states, the power stage can still be controlled.

7.1 Full-Order Output Feedback Integral Control (FOFIC)

Assume the controlled output w is measurable. An $(N + 1)$ -dimensional dynamic controller with output d_n and inputs $y_n \in \mathbf{R}^n$, v_{sn} , and d_n is proposed. To achieve line and load regulation and

to reduce the number of needed state measurements, a controller structure similar to an integrator plus an observer is employed.

The dynamic controller, referred to as full-order output feedback integral control (FOFIC), is

$$v_{n+1} = v_n + W_{\text{SET}} - Ex_n \quad (19)$$

$$z_{n+1} = \Phi_o z_n + \Gamma_d \hat{d}_n + G(y_n - Cx^0(0) - Cz_n) + \Gamma_v \hat{v}_{sn} \quad (20)$$

$$d_n = -K_1 z_n - K_2 v_n \quad (21)$$

where $v_n \in \mathbf{R}$ and $z_n \in \mathbf{R}^N$ are the states of the dynamic controller and $G \in \mathbf{R}^{N \times M}$ is a constant matrix.

From the integrator dynamics in Eq. (19), $Ex^0(0) = W_{\text{SET}}$ in steady state. The output is regulated close to W_{SET} .

Linearizing at the fixed point $(x_n, v_{sn}, d_n, v_n, z_n) = (x^0(0), V_s, d, v, 0)$ gives

$$\begin{bmatrix} \hat{x}_{n+1} \\ \hat{v}_{n+1} \\ z_{n+1} \end{bmatrix} \approx \begin{bmatrix} \Phi_o & 0 & 0 \\ -E & 1 & 0 \\ GC & 0 & \Phi_o - GC \end{bmatrix} \begin{bmatrix} \hat{x}_n \\ \hat{v}_n \\ z_n \end{bmatrix} + \begin{bmatrix} \Gamma_d \\ 0 \\ \Gamma_d \end{bmatrix} \hat{d}_n + \begin{bmatrix} \Gamma_v \\ 0 \\ \Gamma_v \end{bmatrix} \hat{v}_{sn} \quad (22)$$

From the separation property [7] of controller-observer design, it can be proved that the eigenvalues λ of the closed-loop linearized system satisfy

$$(\lambda I - \begin{bmatrix} \Phi_o & 0 \\ -E & 1 \end{bmatrix} + \begin{bmatrix} \Gamma_d \\ 0 \end{bmatrix} \begin{bmatrix} K_1 & K_2 \end{bmatrix})(\lambda I - \Phi_o + GC) = 0 \quad (23)$$

The system is asymptotically stabilizable using the FOFIC method if both of the pairs $(\begin{bmatrix} \Phi_o & 0 \\ -E & 1 \end{bmatrix}, \begin{bmatrix} \Gamma_d \\ 0 \end{bmatrix})$ and (Φ_o, C') are stabilizable. This is generally possible because all the eigenvalues of Φ_o are inside the unit circle.

The feedforward term \hat{v}_{sn} in Eq. (20) can be omitted in this dynamic controller without affecting stability. Adding the feedforward term improves the transient performance.

7.2 Reduced-Order Output Feedback Integral Control (ROFIC)

Similar to the state observer discussed in Section 6, the order of the dynamic controller can be reduced. Without loss of generality, the first M states of the output are assumed to be measurable, so $C = [I, 0]$, where I is an $M \times M$ identity matrix. The state x_n can be partitioned into $[y_n, u_n]$, where u_n is unmeasured state. The matrices Φ_o , Γ_d and Γ_v can also be partitioned accordingly as $\begin{bmatrix} \Phi_{o11} & \Phi_{o12} \\ \Phi_{o21} & \Phi_{o22} \end{bmatrix}$, $\begin{bmatrix} \Gamma_{d1} \\ \Gamma_{d2} \end{bmatrix}$, and $\begin{bmatrix} \Gamma_{v1} \\ \Gamma_{v2} \end{bmatrix}$ respectively. The $(N - M + 1)$ -dimensional dynamic controller with output d_n and inputs y_n , v_{sn} , and d_n is

$$\begin{aligned} v_{n+1} &= v_n + W_{\text{SET}} - E \begin{bmatrix} y_n \\ z_n \end{bmatrix} \\ z_{n+1} &= \Phi_{o22}z_n + \Phi_{o21}\hat{y}_n + \Gamma_{d2}\hat{d}_n \\ &\quad + G(y_{n+1} - Gx^0(0) - \Phi_{o11}\hat{y}_n - \Phi_{o12}z_n - \Gamma_{d1}\hat{d}_n) + \Gamma_{v2}\hat{v}_{sn} \\ d_n &= -K_1 \begin{bmatrix} y_n \\ z_n \end{bmatrix} - K_2v_n \end{aligned}$$

Here v_n and $z_n \in \mathbf{R}^{N-M}$ form the state of the dynamic controller, and $G \in \mathbf{R}^{(N-M) \times M}$ is a constant matrix.

As for the FOFIC method, it can be proved that the eigenvalues λ of the linearized closed-loop system satisfy

$$(\lambda I - \begin{bmatrix} \Phi_o & 0 \\ -E & 1 \end{bmatrix} + \begin{bmatrix} \Gamma_d \\ 0 \end{bmatrix} \begin{bmatrix} K_1 & K_2 \end{bmatrix})(\lambda I - \Phi_{o22} + G\Phi_{o12}) = 0 \quad (24)$$

Thus the closed-loop stabilizability is determined by the stabilizability of the pairs $(\begin{bmatrix} \Phi_o & 0 \\ -E & 1 \end{bmatrix}, \begin{bmatrix} \Gamma_d \\ 0 \end{bmatrix})$ and (Φ'_o, C') and $(\Phi'_{o22}, \Phi'_{o12})$.

8 Illustrative Examples

The *power stage* of the buck converter in [11] is used for the examples in this section. The circuit is shown in Fig. 5. The system parameters are $T = 400\mu s$, $L = 20mH$, $C = 47\mu F$, $R = 22\Omega$, $R_c = 0$ and $V_s = 20V$. Here the focus is on controller design, although the switching frequency is low. The controllers are designed to regulate output voltage (in Example 1 and 2: $W_{SET} = 14V$) or inductor current (in Example 3 and 4: $W_{SET} = 0.7Amp$) under 25% variation of line and load disturbances.

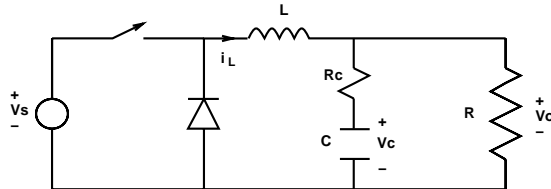


Figure 5: Buck converter with source voltage and resistive load

During the cycle, S_1 is chosen as the off stage and S_2 as the on stage (as in the case of leading-edge modulation). Let the state be $x = (i_L, v_C)$. The state matrices of Fig. 3 are

$$\begin{aligned} A_1 &= A_2 = \begin{bmatrix} 0 & \frac{-1}{L} \\ \frac{1}{C} & \frac{-1}{RC} \end{bmatrix} \\ B_1 &= \begin{bmatrix} 0 \\ 0 \end{bmatrix} & B_2 &= \begin{bmatrix} \frac{1}{L} \\ 0 \end{bmatrix} \end{aligned}$$

In Example 1 and 2, the output voltage is regulated, so $w = v_o$ and $E_1 = E_2 = [0, 1]$. In Example 3, the inductor current is regulated, so $w = i_L$ and $E_1 = E_2 = [1, 0]$.

Example 1 (*Regulation of output voltage to 14V using SFIC*) Since the pair $\left(\begin{bmatrix} \Phi_o & 0 \\ -E & 1 \end{bmatrix}, \begin{bmatrix} \Gamma_d \\ 0 \end{bmatrix} \right)$ is controllable, the eigenvalues can be freely assigned. The magnitude of the control signal depends on the distance between the closed-loop poles and the open-loop poles [7], which are $0.77 \pm 0.2937i$ and 1. To prevent the control signal from being too large, the eigenvalues all at 0.3 are chosen, which results in $K_1 = (-0.00113, -0.0001078)$ and $K_2 = 0.000491$.

Fig. 6 shows the output voltage response during start-up.

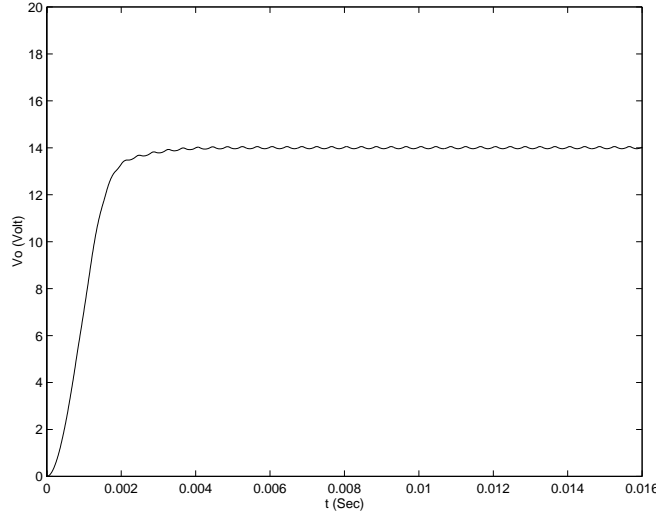


Figure 6: Output voltage response in Example 1 during start-up (SFIC method)

Fig. 7 shows the output voltage response when the source voltage changes to $25V$. As expected, the integral controller reacts promptly and the line regulation is very good.

Fig. 8 shows the output voltage response when the load changes to 16.5Ω . Again as expected, the load regulation is very good.

To show how much this method is an improvement over open-loop control, audio-susceptibility and output impedance are compared with those obtained using open-loop control (with fixed duty ratio 0.7) in Fig. 9 and Fig. 10 respectively.

Example 2 (*Regulation of output voltage to $14V$ using ROFIC*) The closed-loop system diagram is shown in Fig. 11. Here only the output voltage and the source voltage are measured, and input into the dynamic controller. The output voltage is used as a feedback variable, while the source voltage is used as a feedforward variable. The dimension of the dynamic controller is 2. Feedback gains $K_1 = (-1.06 \times 10^{-3}, -8.16 \times 10^{-5})$, $K_2 = 3.61 \times 10^{-5}$, and $G = 0.135$ are chosen to place the eigenvalues of the closed-loop system at 0.4, 0.4, 0.3, and 0.

Fig. 12 shows the output voltage response during start-up.

Fig. 13 shows the output voltage response when the source voltage changes to $25V$. Without the feedforward term from the source voltage, the output voltage can still be regulated with longer

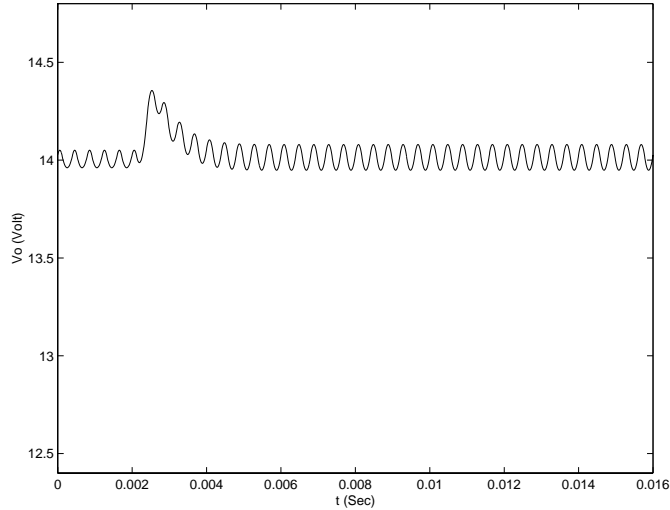


Figure 7: Output voltage response in Example 1 when the source voltage is changed from $20V$ to $25V$ at $t = 0.002s$ (SFIC method)

settling time, as shown in Fig. 14.

Fig. 15 shows the output voltage response when the load changes to 16.5Ω .

Example 3 (*Regulation of peak inductor current to 7Amp using SFIC*) The feedback gains $K_1 = (-0.002, 4.9 \times 10^{-5})$ and $K_2 = 0.0011$ are chosen to assign the closed-loop eigenvalues at 0.2, 0.2 and 0.5. Here the maximum inductor current in *steady state* is regulated. This differs from the traditional current mode control, where the maximum inductor current is *always* below the prescribed limit.

Fig. 16 shows the inductor current response during start-up. The peak inductor current is regulated at $0.7Amp$.

Fig. 17 shows the inductor current response when the source voltage changes to $25V$. Fig. 18 shows the inductor current response when the load changes to 16.5Ω . Under a line or load disturbance, the peak inductor current is always regulated at $0.7Amp$.

Example 4 (*Regulation of average inductor current to 7Amp using SFIC*) Average current can be controlled by adding a low-pass filter. The closed-loop system diagram is shown in Fig. 19. A simple analog low-pass filter, having transfer function $\frac{1000}{s+1000}$, is added to filter the signal of the

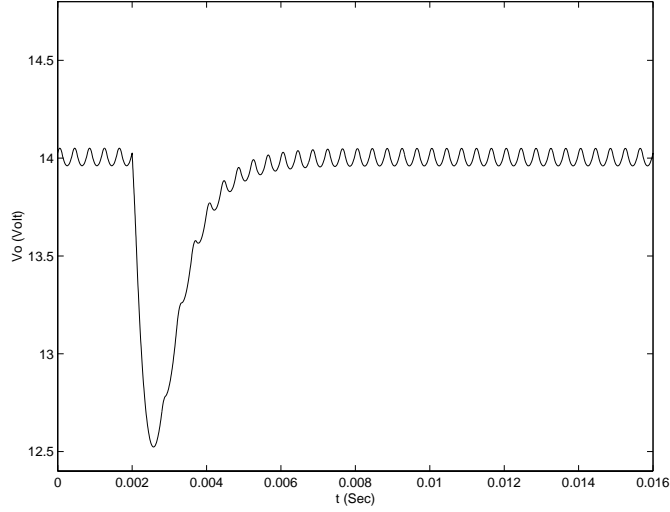


Figure 8: Output voltage response in Example 1 when the load is changed from 22Ω to 16.5Ω at $t = 0.002s$ (SFIC method)

inductor current. This filter raises the dimension of the power stage model from 2 to 3. Let the state be $x = (i_L, v_C, i_f)$, where i_f is the state of the filter. The state matrices in Fig. 3 are

$$\begin{aligned}
 A_1 &= A_2 = \begin{bmatrix} 0 & \frac{-1}{L} & 0 \\ \frac{1}{C} & \frac{-1}{RC} & 0 \\ 1000 & 0 & -1000 \end{bmatrix} \\
 B_1 &= \begin{bmatrix} 0 \\ 0 \\ 0 \end{bmatrix} & B_2 &= \begin{bmatrix} \frac{1}{L} \\ 0 \\ 0 \end{bmatrix} \\
 E_1 &= E_2 = \begin{bmatrix} 0 & 0 & 1 \end{bmatrix}
 \end{aligned}$$

The feedback gains are $K_1 = (-0.00102, -0.000029, -0.00105)$ and $K_2 = 0.0007247$, which assign the closed-loop poles at 0.4, 0.4, 0.3 and 0.7.

Fig. 20 shows the inductor current response during start-up. The *average* inductor current is regulated at $0.7Amp$.

Fig. 21 shows the inductor current response when the source voltage changes to $25V$. Fig. 22 shows the inductor current response when the load changes to 16.5Ω . Under a line or load disturbance, the average inductor current is always regulated at $0.7Amp$.

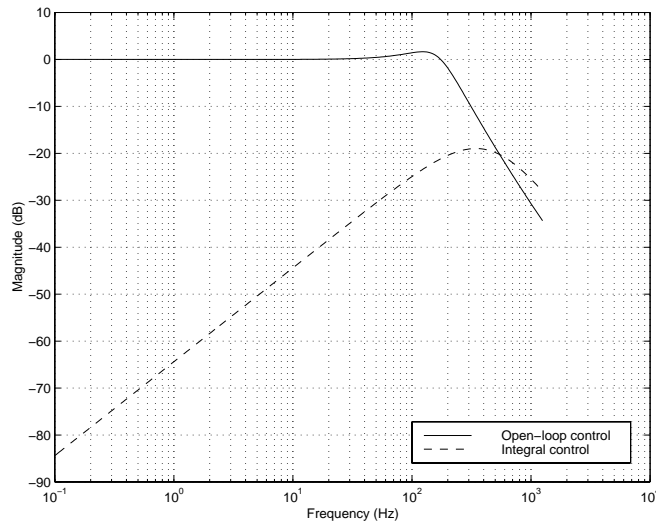


Figure 9: Comparison of normalized audio-susceptibility under open-loop control and state feedback integral control

9 Concluding Remarks

Discrete-time integral control of PWM DC-DC converters has been considered, using recently developed general sampled-data power stage models. Full-order and reduced-order controllers have been introduced. The reduced-order controllers make use of state observers. Several types of control objective can be handled by the method. Simulations were used to illustrate the effectiveness of the design technique.

Acknowledgments

This research has been supported in part by the the Office of Naval Research under Multidisciplinary University Research Initiative (MURI) Grant N00014-96-1-1123, and by the U.S. Air Force Office of Scientific Research under Grant F49620-96-1-0161.

References

- [1] C.-C. Fang and E.H. Abed, “Sampled-data modeling and analysis of PWM DC-DC converters II. The power stage,” preprint, Feb. 1998.
- [2] R.D. Middlebrook and S. Čuk, “A general unified approach to modelling switching-converter power stages,” in *IEEE Power Electronics Specialists Conf. Rec.*, 1976, pp. 18–34.

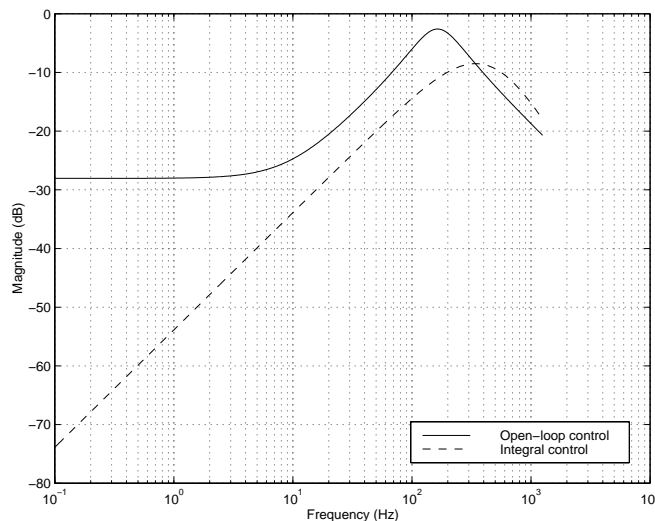


Figure 10: Comparison of normalized output impedance under open-loop control and state feedback integral control

- [3] S. Ćuk and R.D. Middlebrook, “A general unified approach to modelling switching DC-to-DC converters in discontinuous conduction mode,” in *IEEE Power Electronics Specialists Conf. Rec.*, 1977, pp. 36–57.
- [4] R.W. Erickson, *Fundamentals of Power Electronics*, Chapman and Hall, New York, 1997.
- [5] C.-C. Fang, *Sampled-Data Analysis and Control of DC-DC Switching Converters*, Ph.D. thesis, University of Maryland, College Park, 1997.
- [6] A.V. Oppenheim and R.W. Schaffer, *Discrete-Time Signal Processing*, Prentice-Hall, Englewood Cliffs, NJ, 1989.
- [7] T. Kailath, *Linear Systems*, Prentice-Hall, Englewood Cliffs, NJ., 1980.
- [8] A.K.S. Bhat, “Fixed frequency PWM series-parallel resonant converter,” in *Conference Record of the IEEE Industry Applications Society Annual Meeting*, 1989, pp. 1115–1121.
- [9] L.A. Kamas and S.R. Sanders, “Parameter and state estimation in power electronic circuits,” *IEEE Transactions on Circuits and Systems-I: Fundamental Theory and Applications*, vol. 40, no. 12, pp. 920–928, 1993.
- [10] P. Midya, *Nonlinear Control and Operation of DC to DC Switching Power Converters*, Ph.D. thesis, University of Illinois, Urbana-Champaign, 1995.
- [11] D.C. Hamill, J.H.B. Deane, and J. Jefferies, “Modeling of chaotic DC-DC converters by iterated nonlinear mappings,” *IEEE Transactions on Power Electronics*, vol. 7, no. 1, pp. 25–36, 1992.

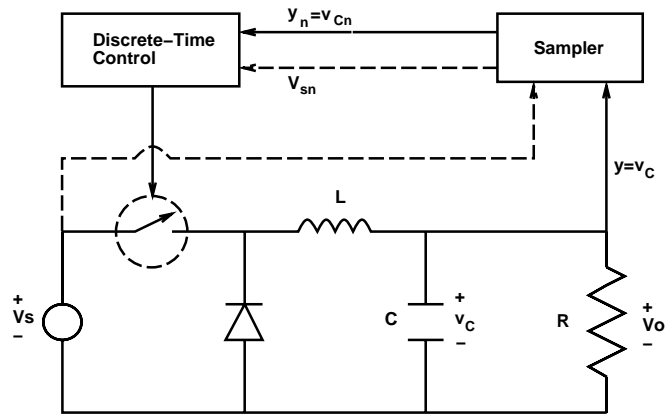


Figure 11: Closed loop system diagram using ROFIC

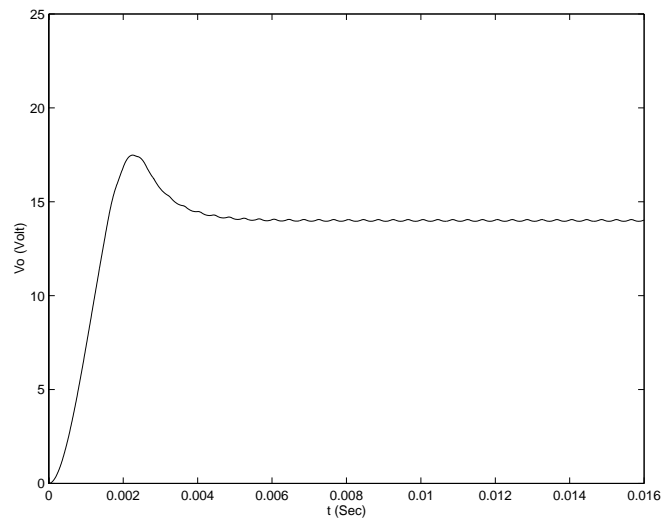


Figure 12: Output voltage response in Example 2 during start-up (ROFIC method)

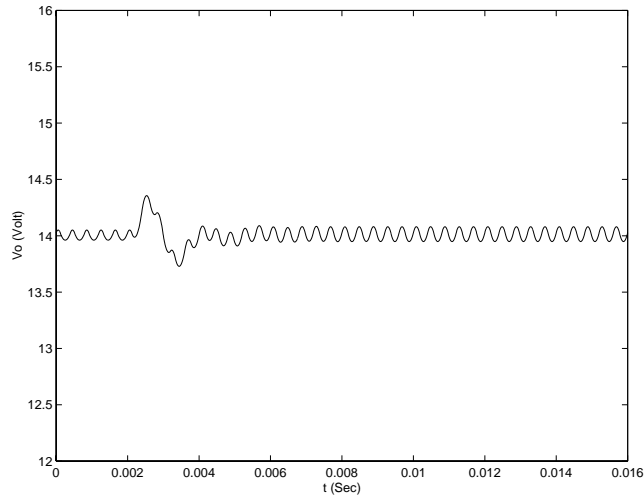


Figure 13: Output voltage response in Example 2 when the source voltage is changed from $20V$ to $25V$ at $t = 0.002s$ (ROFIC method)

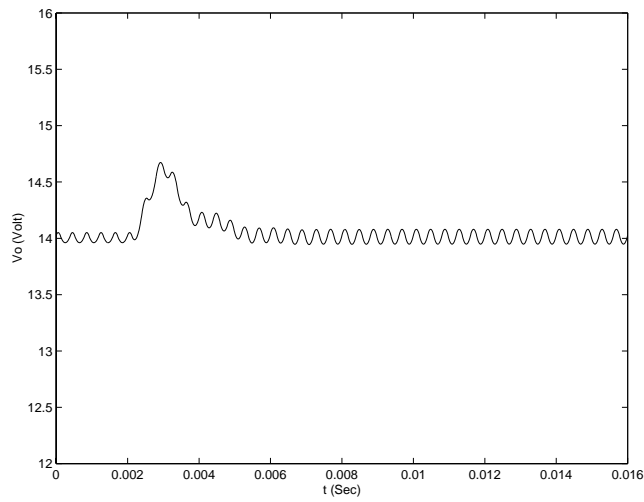


Figure 14: Output voltage response in Example 2 when the source voltage is changed from $20V$ to $25V$ at $t = 0.002s$ (ROFIC method without source voltage feedforward)

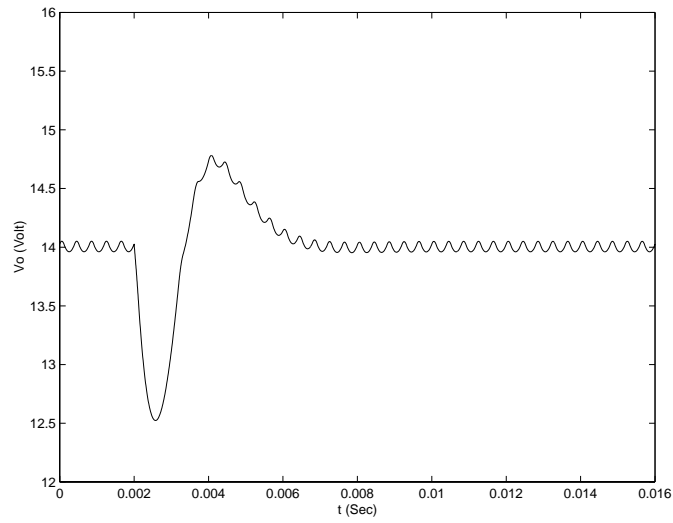


Figure 15: Output voltage response in Example 2 when the load is changed from 22Ω to 16.5Ω at $t = 0.002s$ (ROFIC method)

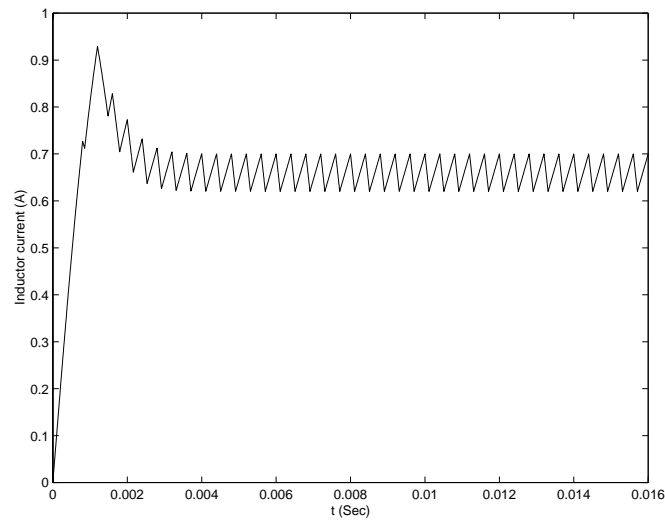


Figure 16: Inductor current response in Example 3 during start-up (SFIC method)

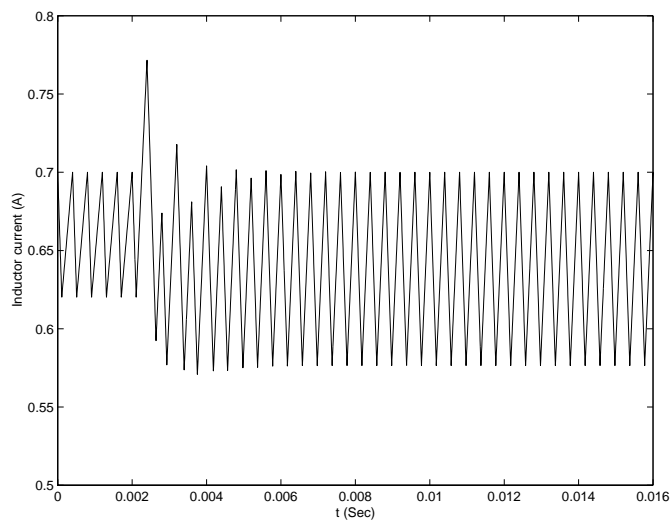


Figure 17: Inductor current response in Example 3 when the source voltage is changed from $20V$ to $25V$ at $t = 0.002s$ (SFIC method)

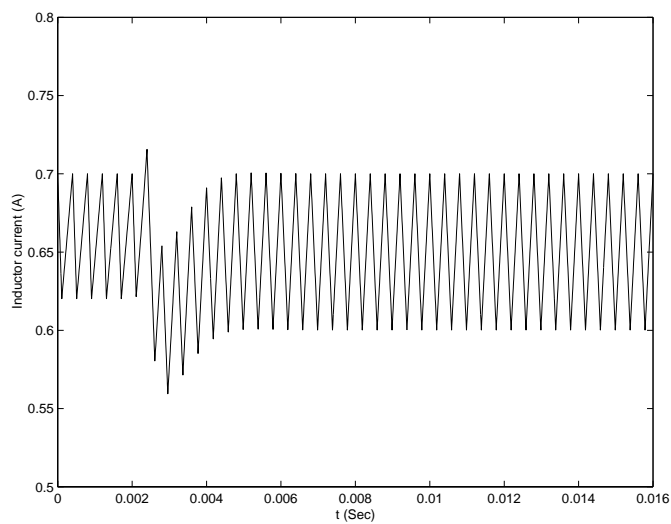


Figure 18: Inductor current response in Example 3 when the load is changed from 22Ω to 16.5Ω at $t = 0.002s$ (SFIC method)

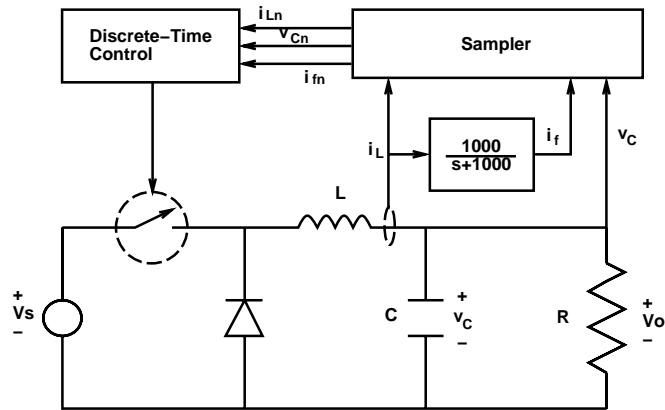


Figure 19: System diagram of average inductor current control in Example 4

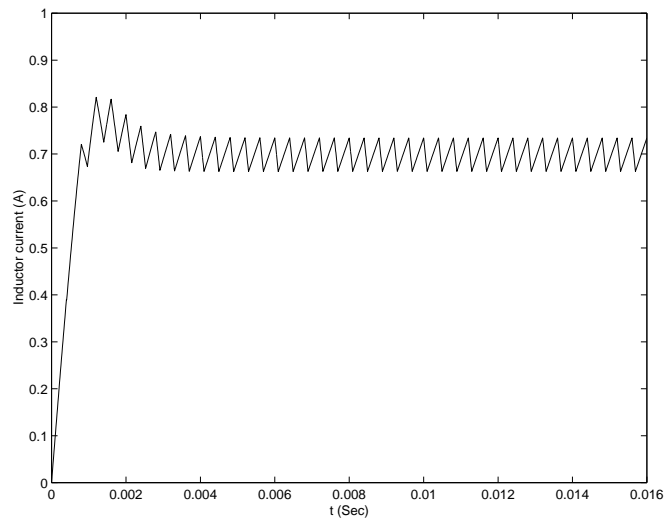


Figure 20: Inductor current response in Example 4 during start-up (SFIC method)

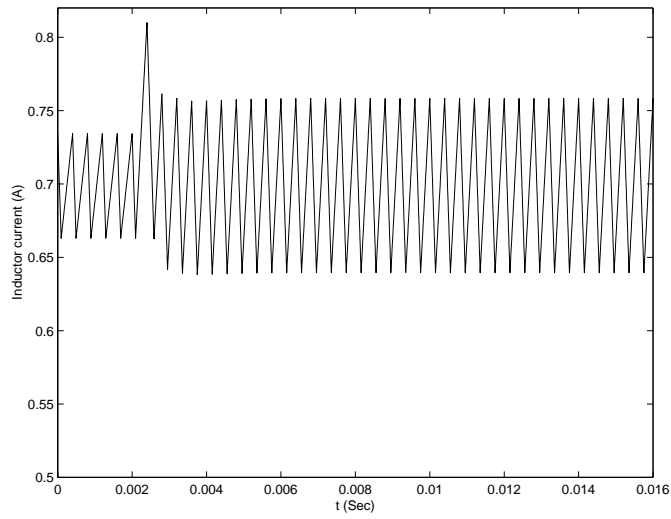


Figure 21: Inductor current response in Example 4 when the source voltage is changed from $20V$ to $25V$ at $t = 0.002s$ (SFIC method)

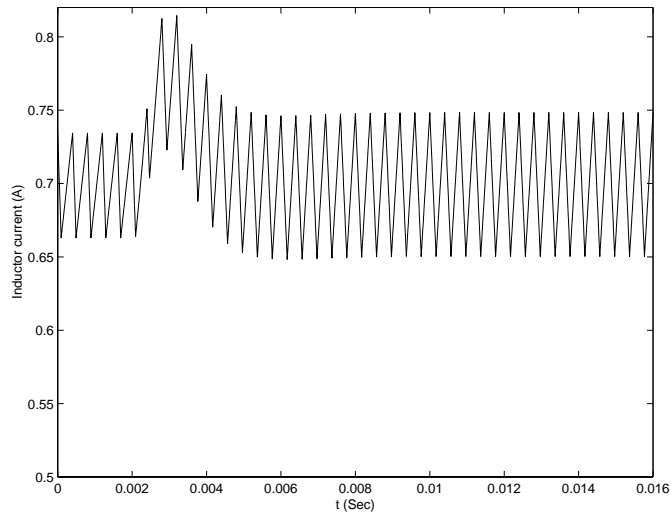


Figure 22: Inductor current response in Example 4 when the load is changed from 22Ω to 16.5Ω at $t = 0.002s$ (SFIC method)